In W.E. Krumbein, D. Paterson & G. Zavarzin (2003), Fossil and recent biofilms, a natural history of life on planet Earth. Kluwer Academic Publishers, Dordrecht.

Chapter 5

GROWTH, STRUCTURE AND CALCIFICATION POTENTIAL OF AN ARTIFICIAL CYANOBACTERIAL MAT

Michael KÜHL and Tom FENCHEL
Marine Biological Laboratory, University of Copenhagen
Strandpromenaden 5, DK-3000 Helsingør, Denmark.
mkuhl@zi.ku.dk

Jozef KAZMIERCZAK
Institute of Paleobiology, Polish Academy of Sciences,
Biogeology Division, Twarda 51/55, PL 00-818 Warszawa, Poland

1. INTRODUCTION

Microbial mats growing on and within light-exposed surfaces harbor complex structured microbial communities of both aerobic, microaerophilic and anaerobic microbes, which in their concerted action exhibit almost closed cycles of carbon, sulfur and other essential elements for biological growth and development (Canfield and Des Marais 1993; van Gemerden 1993; Stal 2000). Diatoms and, primarily, cyanobacteria constitute the major primary producers in most microbial mats. Anoxygenic photosynthetic bacteria (both photoautotrophs and photoheterotrophs) are also abundant, but their contribution to the primary production of mats is regarded minor (Canfield and Des Marais 1993), with the exception of certain hot spring mats (Jørgensen and Nelson 1988) and coastal mats of purple bacteria (van Gemerden *et al.* 1989). Due to the absence or very minor presence of higher organisms (macrophytes and animals), microbial mats represent well developed microbially driven ecosystems. In extreme environments, like in hypersaline or geothermal waters, microbial mat communities are relatively stable over time periods >1 year and they can develop into cm to m thick

cohesive layers consisting of >90% exopolymer and cells (e.g. Krumbein *et al.* 1977; Jørgensen *et al.* 1983; DesMarais 1995). Coastal mats in temperate environments are thinner and have a more ephemeral occurrence (Stal *et al.* 1985; van Gemerden *et al.* 1989). Intertidal microbial mats play an important role for coastal morphology due to their sediment binding and stabilization properties (Krumbein *et al.* 1994). In special aquatic environments, like alkaline lakes and tropical intertidal and subtidal zones, sediment trapping by microbial mats in combination with calcification leads to formation of conspicuous solid structures like beachrock lining the intertidal of tropical lagoons (Krumbein 1979b), and laminated cushion (Logan 1961; Dravis 1983; Riding *et al.*1991; Reid *et al.* 2000) and dome shaped (Kempe *et al.* 1991) structures interpreted as living stromatolites.

Microbial mats are ideal model systems for studying the interaction and regulation of microbial life and its biodiversity. Furthermore, some microbial mats are regarded as recent analogues of stromatolites, the earliest signs of biotic communities on Earth that are preserved in the fossil record, and which exhibit a striking similarity in both macro- and microstructure to some of the present microbial mats (Grotzinger and Knoll 1999; Schopf and Klein 1992). This has been inferred from (Schopf 2000): i) an impressive structural similarity between preserved microfossils and microorganisms, especially cyanobacteria, present in recent microbial mats, and ii) comparative geological and geochemical studies of fossil and recent microbial mats. Thus, microbial mat studies not only gain fundamental principles and mechanisms of today's microbial ecology, they also allow to infer and test hypotheses on how the earliest ecosystems on Earth may have evolved and functioned. However, many, if not most, extant microbial mats do not lead to stromatolite formation (see e.g. Stal 2000) and extrapolation from studies of recent mats to Precambrian analogues should be done with care.

Most microbial mat studies have been done with natural mats either *in situ* or with samples transferred to the laboratory. Much less effort has been made to induce and study microbial mat growth in the laboratory, in part due to the difficulty to create and maintain the multitude of gradients (light, oxygen, pH, inorganic carbon, nutrients etc.) driving the organization and activity within microbial mats. Giani *et al.* (1989) described a laboratory scale device for growing hypersaline microbial mats, which was later adapted for a number of different model systems for studying intertidal microbial mats (Krumbein *et al.* 1994, pp. 492-497). A mesocosm facility for studying hypersaline microbial mats has been established at the Interuniversity Institute in Eilat, Israel by Yehuda Cohen (see http://www.univ-pau.fr/RECHERCHE/MATBIOPOL/; Abed and Garcia-Pichel 2001), and a controlled greenhouse facility for hypersaline microbial mats has been established by the NASA exobiology section in Palo Alto, California

(http://exobiology.nasa.gov/microecobiogeo/html_documents/greenhouse_one.htm; Bebout et al. 2002). A benchtop system for growing artificial microbial mats in defined gradients has been developed by Pringault *et al.* (1996), and has been used extensively to study artificial mats of anoxygenic photosynthetic bacteria (Pringault *et al.* 1999a,b) and cyanobacteria (Pringault and Garcia-Pichel 2000).

The mentioned systems have mostly relied on inoculation with natural mat samples or defined cultures of phototrophic microorganisms and involved elaborate controls of environmental parameters. An alternative and simple approach was invented by Fenchel (1998a), who induced prolific microbial mat growth on top of natural coastal sediment, by experimental removal of fauna. In this chapter we review the development, structure and function of these artificially induced cyanobacterial mats, including an account of their calcification potential.

2. GRAZING AND FORMATION OF ARTIFICIAL CYANOBACTERIAL MATS

The effect of grazing on microbial mats has been studied in both hypersaline and geothermal microbial mats (reviewed by Farmer 1992). The presence of grazers does not always imply destruction of mats (McNamara 1992), and the presence of grazers can significantly affect both the diversity of phototrophs and mat structure.

In hypersaline environments insect (coleopteran and dipteran) larvae and nematodes are predominant grazers of diatoms and cyanobacteria (Gerdes *et al.* 1985; Farmer 1992), especially in mats with heterogeneous surface structures (Gerdes and Krumbein 1987). However, abundant grazing meiofauna and small crustaceans like the harpacticoid copepod *Cletocampus dietersi* seem to have little impact on hypersaline mat distribution (Farmer 1992). Cerithid gastropods (e.g. *Cerithidia californica*), the waterboatman *Trichocorix sp.*, and salt beetles (*Bledius* spp. adults and larvae) are larger conspicuous grazers of hypersaline mats (Javor and Castenholz 1984; Gerdes and Krumbein 1987). Even mat reworking by crabs and grazing fish are reported (Davies 1970; Schwarz *et al.* 1975)

Grazing larvae of the brine fly *Paracoenia turbida* can control mat development in hot springs at <40°C (Wickstrom and Wiegert 1980). Thermophilic ostracods (*Potamocypris* sp.) have been shown to facilitate, by selective grazing, the co-occurrence of two competing cyanobacteria (*Calothrix thermalis* and *Pleurocapsa minor*) in nodular mats in hot springs (Wickstrom and Castenholz 1985). Overgrowth of the nodular mat by more efficiently growing *Synechococcus* and *Oscillatoria* mats was prevented by

ostracod grazing at temperatures below 47-51°C, i.e. the upper temperature limit of the ostracod population.

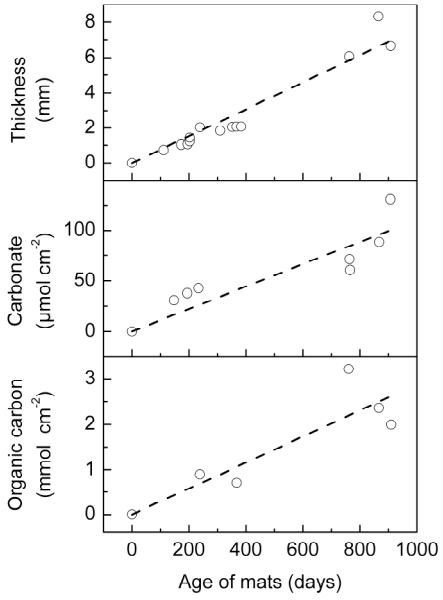

Figure 1. Increment of thickness, carbonate and organic carbon content of the artificial mats as a function of time (from Fenchel and Kühl 2000)

The role of grazers for microbial mat formation and destruction in temperate systems was studied by Fenchel (1998a). Formation of microbial mats was induced by removal of macro- and most meiofauna in coastal sediment by 20h freezing at –20 °C, and subsequent incubation in sterile seawater at constant temperature under a 10h dark-14h light cycle. Within 3-4 weeks after defaunation a cyanobacterial mat was formed on top of the sediment, which over the following 4-5 years has developed further into a complex laminated microbial mat with an accretion rate of ~2-3 mm per year, a carbonate accumulation rate of ~0.3 µmol cm^{-2} d^{-1}, and an accumulation rate of organic carbon of ~2.5 µmol cm^{-2} d^{-1} (Fenchel and Kühl 2000, Fig. 1). The accretion rates of natural hypersaline microbial mats are in the range of 0.5-5 mm per year (Bauld 1981, DesMarais 1995).

The presence of resistant meiofauna and a harpacticoid copepod *Harpacticus* sp. did not affect mat development. However, when fauna (the harpacticoid copepod *Nitocra* sp., hydrobiid snails and polychaetes) was allowed to recolonize ~4 months old mats, the mat was digested within ~2 weeks and the laminated structure changed into bioturbated sediment (Fenchel 1998a, Fig. 2B). It was concluded that normal sediments bear a

potential for microbial mat formation (similar to the ones found in extreme habitats), which is, however, only realized when faunal grazing and bioturbation is depressed. These observations are interesting in the context that the origin of metazoan life, and therefore benthic fauna, apparently coincided with the decline of late Precambrian stromatolites (Garret 1970; Walter and Heys 1985), and the fact that most modern stromatolites occur under environmental conditions that restrict metazoan life.

2.1 Changes in structure, biota and diversity

The development of the artificial cyanobacterial mats was followed intensively over the first year of mat development (Fenchel 1998a,b, c). Another detailed investigation was done with 2-2.5 year old mats (Fenchel and Kühl 2000; Kühl and Fenchel 2000). On both occasions a very detailed study of mat structure and composition was done with TEM, and biovolumes were determined by stereological methods.

2.1.1 The first year after defaunation

Within 4 months after defaunation, the mats had developed into a laminated cohesive yellow-brownish matrix of cells and exopolymers, with different phototrophs dominating in different strata (Fenchel 1998b). Calcification was evident from the formation of carbonate precipitates within the cyanobacterial zone 0.2-0.3 mm below the mat surface. Both chlorophyll *a* and bacteriochlorophyll *a* concentrations increased during this period and reached levels of ~140 µg Chl *a* cm^{-2} and 20 µg Bchl *a* cm^{-2} (Fig. 2). A prominent feature was the presence in the upper 3 mm's of the mat of several layers densely populated by filamentous cyanobacteria (mainly two morphotypes of *Pseudanabaena*). Layers with vertical filament orientation were sharply separated from layers where filaments were oriented in parallel to the surface and each other. Maximum volume fractions of filamentous cyanobacteria were ~10-15% (25-30% with slime sheaths) in these layers. The total length of cyanobacterial filaments below 1 cm^2 of mat was estimated to ~14 km at this stage of development. Photosynthetic bacteria were relatively sparse and mainly confined to a layer with *Thiocapsa* colonies ~4-5 mm below the surface. Bacterial biomass accounted for ~2% of the volume in the uppermost 0.2-0.3 mm (~5 x 10^{10}) of the mat and ~0.5% in deeper layers (~5 x 10^9 bacteria ml^{-1}). Bacterial density tended to vary with cyanobacterial density, and bacteria were observed to also colonize the outer and inner surfaces of cyanobacterial sheaths.

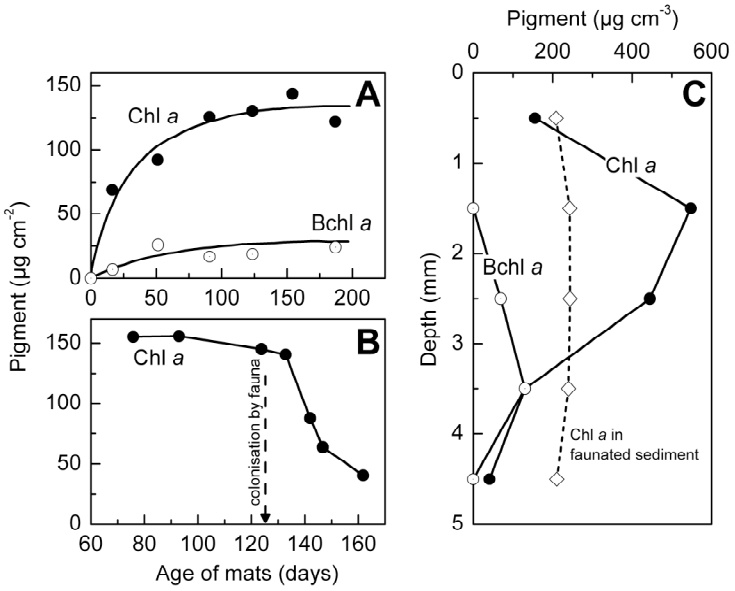

Figure 2. Accumulation of photopigments during mat development (A), and degradation after colonization by fauna (B). Depth distribution of photopigments in an artificial mat and in a faunated sediment (C) (from Fenchel 1998a).

While the mat structure and density of microorganisms was similar to that of natural cyanobacterial mats, the diversity of phototrophs was apparently lower than in natural mats (Nübel *et al.* 1999). Besides the dominating *Pseudanabaena* spp., minor occurrence of coccoid morphotypes and filamentous forms assigned to *Phormidium*, *Microcoleus* and *Calothrix* was found.

2.1.1.1 Later stages of development

Approximately 2-2.5 years after defaunation, *Microcoleus* had disappeared and *Phormidium* and *Calothrix* were more numerous in the upper 1 mm of the mat (Fenchel and Kühl 2000). Three morphotypes of *Pseudanabaena* were still the most abundant cyanobacteria. The stratification observed in young mats was preserved, but zonations in the older mat were more pronounced with a complex texture, and biovolumes were somewhat higher (Fenchel and Kühl 2000). It was estimated that the filamentous cyanobacteria below a cm^2 of mat represented a surface area of ~350 cm^2. The diversity

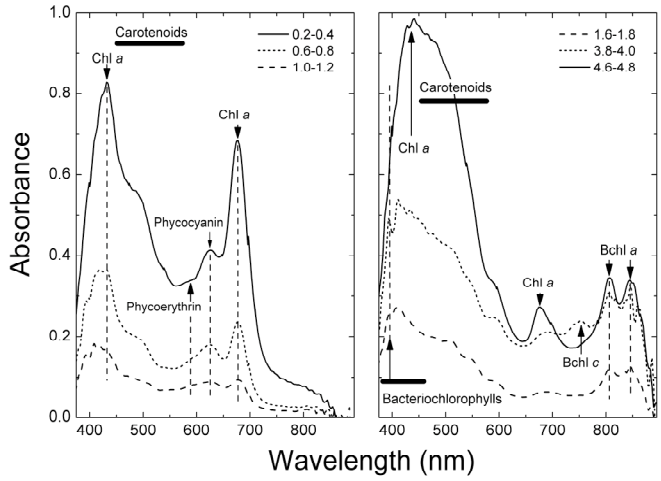

Figure 3. Spectral absorbance of various zones (denoted by depth intervals in mm) as measured by microscope spectrometry on vertical thin sections of an artificial mat (from Kühl and Fenchel 2000).

and abundance of photosynthetic bacterial layers with different photopigments was somewhat increased (Fig. 3). Several carbonate layers were present. A dense 0.2-0.4 mm thick layer of carbonates within the upper mm of the mat, a second less dense carbonate layer 1.5-2 mm below the surface, and sometimes a third layer in-between purple bacteria 3-5 mm below the mat surface. Carbonate precipitates associated with cyanobacterial sheaths were observed. The largest part of the mat was composed of empty cyanobacterial sheaths and exopolymers. The sheaths appear resistant to degradation and their accumulation seems the major cause for the slow increase in mat thickness over time (Fig. 1A). The mats continue to develop in the mesocosms, and most recently conspicuous gelatinous pinnacle structures have developed on the mat surface (Fig. 4).

Besides a stratification of cyanobacteria and anoxygenic phototrophic bacteria (Fig. 3), the mat structure exhibits 3 prominent characteristics found in extant natural mats and often interpreted as preserved in fossil material (Bauld *et al.* 1992): i) a pronounced microfabric of cyanobacterial lamina, where layers with vertical filament orientation are separated from layers with pronounced horizontal filament orientation, ii) abundance of empty cyanobacterial sheaths, which are not mineralized and together with exopolymers constitute the bulk mass of the mats, and iii) presence of distinct layers of carbonate precipitates associated with zones of high photosynthesis and zones of mainly heterotrophic activity.

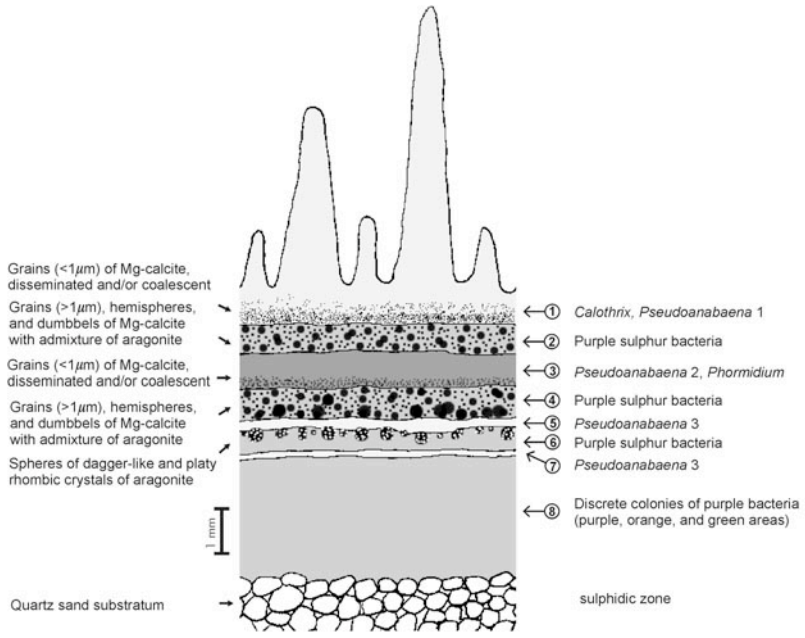

Figure 4. The vertical micro-zonation in a ~3 year old artificial cyanobacterial mat. Different characteristic zonations of phototrophs are numbered and referred to in the text. The location of calcium carbonate precipitates is indicated with arrows. Detailed LM and TEM pictures of the mats in earlier stages of development can be found in Fenchel (1998a, b) and in Fenchel and Kühl (2000). The prominent pinnacles developed within the last 12-18 months and were absent or only minor in the earlier stages of development.

3. MICROENVIRONMENTAL CHARACTERISTICS AND CARBON CYCLING

Besides a high structural similarity, the carbon cycling and microenvironmental characteristics of the artificial mat (Fenchel 1998c, Kühl and Fenchel 2000) are very similar to results obtained in natural marine mats found in hypersaline environments (e.g. Revsbech *et al.* 1983; Jørgensen 1989; Canfield and Des Marais 1993; Des Marais 1995; Wieland and Kühl 2000).

3.1 Physical and chemical microenvironment

Fiber-optic microprobes for field radiance and scalar irradiance (Kühl et al. 1994) were used for measurements of i) depth distribution of chl *a* and phycobilin fluorescence (Thar et *al.* 2001), ii) depth distribution of available light for oxygenic photosynthesis, PAR, (Kühl *et al.* 1997). Electrochemical microsensors for O_2, pH, S_{2-}, and H_2S (Kühl and Revsbech 2001) were used to quantify oxygen and sulfide dynamics in the mats.

Oxygen and sulfur cycling was closely coupled in ~4-12 months old artificial mats (Fenchel 1998c). Oxygen penetration varied from 0 in darkness to ~2.5 mm in light, where photosynthesis in a ~1 mm thick photic zone created O_2 super-saturation within the mat. In darkness, sulfide oxidation could account for all oxygen consumed and mineralization was entirely anaerobic with sulfate as the terminal e--acceptor. The main source of sulfide was in the reduced sediment below the mat but sulfate reduction was also found in the uppermost 1 mm of the mat, corresponding to the photic zone. In light, sulfide was removed by anoxygenic photosynthesis in the mat and sulfide was only present in the deepest mat layers (>3 mm). It was estimated that anoxygenic photosynthesis accounted <10% of primary production.

In ~2-2.5 year old mats, sulfide was only present below the 4-5 mm thick oxic zone in the light, and O_2 penetration in the dark was ~1 mm, allowing for some aerobic mineralization in the uppermost layers of the mat (Fig. 5). pH in the photic zone varied from pH 8.8 in light to pH 8.3 in darkness. Strong attenuation of visible light confined the zone of oxygenic photosynthesis to the upper 3 mm's of the mat. Oxygenic photosynthesis, light attenuation and photopigment fluorescence showed a heterogeneous depth distribution with several peaks corresponding to the different layers of cyanobacteria carbonate precipitates (Fig. 6). Scattering in the matrix of exopolymers, carbonate precipitates, and cells resulted in a local maximum in scalar irradiance in the upper 0.2-0.5 mm of the mat.

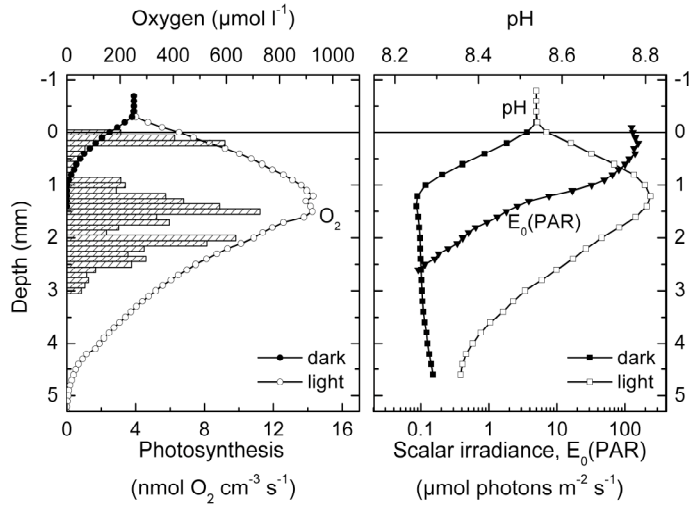

Figure 5. Microprofiles of O2, pH, scalar irradiance (E0(PAR), and gross oxygenic photosynthesis (bars) in a ~2.5 year old 7-8 mm thick artificial mat. Incident irradiance in light was 413 µmol photons m^{-2} s^{-1} (from Kühl and Fenchel 2000).

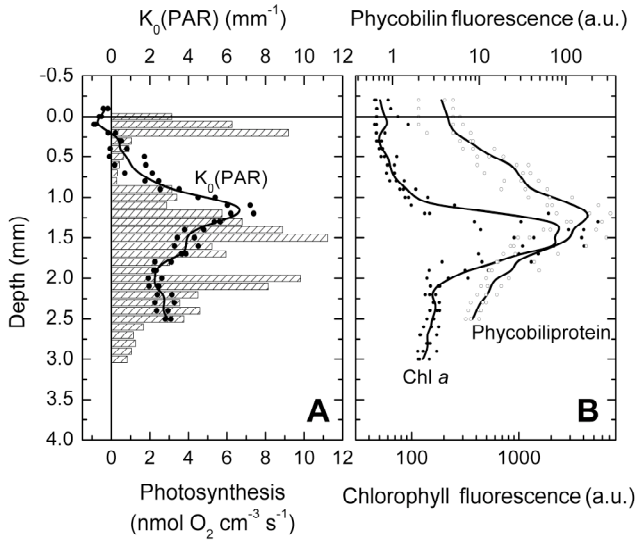

Figure 6. Depth dependence of (A) oxygenic photosynthesis (bars) and scalar irradiance attenuation, and (B) chlorophyll *a* and phycobiliprotein fluorescence in a ~2.5 year old and 7-8 mm thick artificial mat (from Kühl and Fenchel 2000).

3.2 Cycling of carbon and other elements in the mats

Net uptake (1.244 ± 0.305 μmol cm^{-2} h^{-1}) in light and net production (1.235 ± 0.236 μmol cm^{-2} h^{-1}) in dark of inorganic carbon were almost identical in the mat (Fenchel 1998c). This is in accordance with the slow accumulation of organic carbon (estimated to ~10% of net C fixation) within the mats (Fig. 1), and points to an efficient recycling of carbon, sulfur, oxygen and other elements in the mat.

Chemotrophic and photosynthetic sulfur bacteria reoxidized most sulfide produced by sulfate reduction. The dynamics of sulfide was, however, buffered by a pool of intermediate oxidation products like elemental sulfur (S^0) and of iron sulfide (FeS) temporary immobilizing some of the free sulfide. Permanent burial of sulfide as pyrite (FeS_2) was not measured but is probably low in the artificial mats. Carbonate precipitation was estimated to ~1% of inorganic carbon uptake and most probably is stimulated by the high pH of ~9 found in the photic zone during illumination (Fig. 5, see also 4).

Net oxygen fluxes in light and darkness did not balance and were 2-3.5 times lower than the corresponding inorganic carbon fluxes. In the light, oxygen is also used to reoxidize i) reduced pools of carbon and sulfur accumulating during darkness, and ii) reduced storage products accumulating in the cyanobacteria during illumination periods. Furthermore, oxygen respiration within the photic zone is also stimulated in light due to excretion of photosynthates by the cyanobacteria, which are surrounded by a high density of heterotrophic bacteria. Whether this apparent cross-feeding of heterotrophs, often observed in mats (e.g. Canfield and Des Marais 1993; Kühl *et al.* 1996; Paerl *et al.* 2000), also results in significant CO_2 transfer to the cyanobacteria is unknown, but together with carbonate precipitation in the vicinity of the cyanobacteria this could help alleviate inorganic carbon limitation induced by the high pH in the photic zone.

4. CALCIFICATION POTENTIAL OF THE ARTIFICIAL CYANOBACTERIAL MATS

The mechanism of calcification in cyanobacterial mats, and the use of such information as a key to elucidate the origin of ancient sedimentary structures known as stromatolites, and of other carbonate deposits interpreted as products of calcified benthic cyanobacteria (Kazmierczak *et al*. 1996; Riding 2000), are still poorly understood and controversial (Krumbein 1979a; Ginsburg 1991; Grotzinger and Knoll 1999; Reid et al. 2000). Hence, the possibility to study $CaCO_3$ precipitates in well-

characterized artificial cyanobacterial mats offers new insights to the origin of $CaCO_3$ deposits, but also to the genesis of their fossil counterparts.

4.1 Distribution and morphology of $CaCO_3$ precipitates

First $CaCO_3$ precipitates appeared in the mats ~2 months after defaunation of the original sediment (Fenchel 1998a). After 4 months $CaCO_3$ deposits occurred as 100-200 μm large white granules, which in ~1 year old mats had grown together to form an almost continuous, but perforated, 100-200 μm thick plate (cf. Fig. 1F in Fenchel 1998a). After ~2 years growth, a second carbonate layer had been generated in the mats (Fenchel and Kühl 2000). The carbonate precipitates were investigated with cryo-microtome sectioning techniques, scanning electron microscopy (SEM), X-ray diffractometry (XRD), electron microprobe analysis (EDS), and stable carbon isotope ratio measurements ($\delta^{13}C$). The basis for these studies were ~2 year old mats. Selected control analyses were carried out on carbonates in ~3 year old mats.

The results of morphological and mineralogical investigations of the $CaCO_3$ particles identified in the mat vertical section are summarized in Fig. 4. They are based on cryo-microtome sections (Fig. 7A) and SEM images of the $CaCO_3$ precipitates occurring in particular biozones (Figs. 7B-E, 9, and 10). The distribution of $CaCO_3$ precipitates within the mats was non-random and associated to particular microzones (numbered in Fig. 4). Several carbonate layers could be distinguished in the ~7 mm thick mat beginning from their pinnacled uppermost biozone down to the sandy sulfidic substratum.

At the basis of the uppermost biozone composed of *Calothrix* and *Pseudanabaena* 1 (zone 1 in Fig. 4; Fig. 7 A1) an almost continuous dense layer of spherical/subspherical submicron-sized $CaCO_3$ grains occurred. The grains were distributed both on the slime sheaths of living cyanobacterial filaments and within the extracellular polymers (EPS) surrounding the sheaths. The 50-750 nm-sized particles occurred either as irregular individual bodies or as loosely coalesced chain-like groups (Fig. 7B). Larger clusters of similar particles were occasionally observed (Fig. 7C). X-ray diffractometry showed that this carbonate layer was composed exclusively of high Mg-calcite enclosing 15-17 mole% $MgCO_3$ (Fig. 8, curve *a*). Interestingly, electron microprobe analysis (EDS) revealed that in the ~3 years old mats the same layer now also contained a mixture of amorphous magnesium silicates.

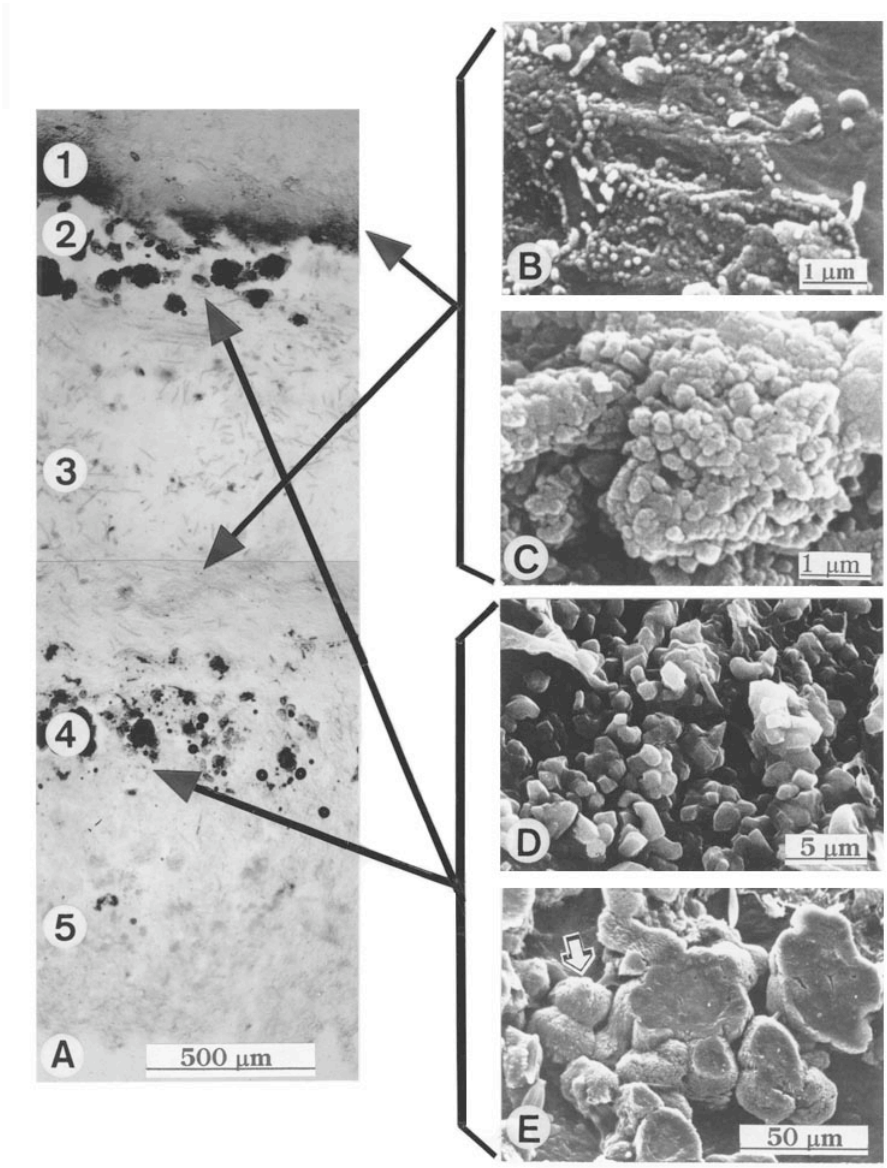

Figure 7. (A) Vertical cryotome section of a ~2 year old mat showing the location of $CaCO_3$-rich layers (arrows). Numbers indicate particular layers corresponding to those marked in Fig. 4. (B, C) Submicrometer-sized Mg-calcite grains dispersed (B) or forming clusters (C) at the bottom of the living cyanobacterial layer (zones 1 and 3). (D) Larger (>1µm) anhedral and subhedral grains of Mg-calcite from zones 2 and 4. (E) Hemispheres and dumbbells (arrow) of Mg-calcite with admixture of aragonite found in zones 2 and 4.

In the underlying biozone composed of purple sulfur bacteria and heterotrophic bacteria (zone 2 in Fig. 4) and separated from the top cyanobacterial zone by a sharp boundary, a carbonate layer with much larger anhedral and subhedral 2-4 µm sized $CaCO_3$ grains occurred (Fig. 7 A2). The grains showed a tendency to develop crystal faces (Fig. 7D), button-like 20-110 µm large hemispheres (Fig. 7E; Fig. 9A-B), as well as 20-50 µm long peanut- and dumbbell-like bodies (Fig. 7E; Fig. 9A, C, D). The hemispheres were often coalesced into larger plate-like structures. X-ray diffractometry of the layer showed up to 90% of high Mg-calcite (with ~15 mole % $MgCO_3$) and ~10% aragonite (Fig. 8, curve *b*). The carbonate particles in this zone were often entangled in felt-like remnants of strongly degraded cyanobacterial sheaths.

A distinct deep green colored cyanobacterial layer composed of filaments of *Pseudanabaena* 2 and *Phormidium* (zone 3 in Fig. 4; Figs. 7A, 9) was found in deeper mat layers. At the base of this zone a carbonate layer comprised of ultra small high Mg-calcite particles occurred on the cyanobacterial sheaths and in the EPS. The particles were practically identical with those from the base of the uppermost layer, although the density of their distribution was much lower (compare Figs. 7A, 9).

In a deeper zone with purple sulfur bacteria (zone 4 in Fig. 4), a layer of relatively large carbonate particles occurred (Figs. 7A, 9). The particles comprised >1 µm large anhedral and subhedral grains, many with well-developed crystal faces, button-like hemispheres and dumbbell-like bodies. There were many imperfect peanut shaped particles, which were particularly numerous in places rich in felt-like remnants of degraded cyanobacterial sheaths (Fig. 9C, D). Like in zone 2, the carbonate particles in this layer were composed of high Mg-calcite with admixture of aragonite.

The deepest located carbonate bodies occurred in a zone of purple sulfur bacteria (zone 6 in Fig. 4) located between two thin zones composed of *Pseudanabaena* 3 (zones 5 and 7 in Fig. 4). The carbonate precipitates were 50-120 µm wide spherical and sub-globular aggregates composed of i) dagger-like crystals (Fig. 10A, B), which resembled trigonal prism crystallites described by Given and Wilkinson (1985), or ii) sub-globular aggregates of platy-rhombic crystals bearing a character of trigonal prisms with rhombic termination (Fig. 10C, D). Aggregates of dagger-like crystals and rhombic plates were relatively rare and most of them were aragonitic, sometimes with small amounts of high Mg-calcite.

4.2 The origin of calcium carbonate precipitates

Saturation indices calculated with respect to calcite, aragonite, and dolomite showed very high supersaturation values in the uppermost 2-3 mm's of the mat. The high values were due to high pH and carbonate alkalinity levels generated by microbial metabolism in the mats and to increased concentration of Ca^{2+} and Mg^{2+} liberated from decaying Ca- and Mg-enriched cyanobacterial sheaths and exopolymers. The mode of occurrence of calcium carbonate precipitates in the studied mats indicates two different processes involved in their formation within two different microbial zones:

4.2.1 Calcium carbonate precipitation in vicinity of living cyanobacteria.

Precipitation of ultra small high Mg-calcite grains was found in the cyanobacterial layers of biozones 1 and 3 (Fig. 4). The nucleation and precipitation of calcium carbonate deposits on and/or within the mucus sheaths surrounding living cyanobacteria is a spontaneous process resulting from the high pH induced by photoassimilatory uptake of CO_2 and/or HCO_3^-, and the resulting increase in saturation level with respect to the solubility product of common calcium carbonate minerals (Pentecost and Bauld 1988; Merz 1992; Merz and Zankl 1993; Ferris *et al*. 1994, 1997; Schultze-Lam *et al*. 1996).

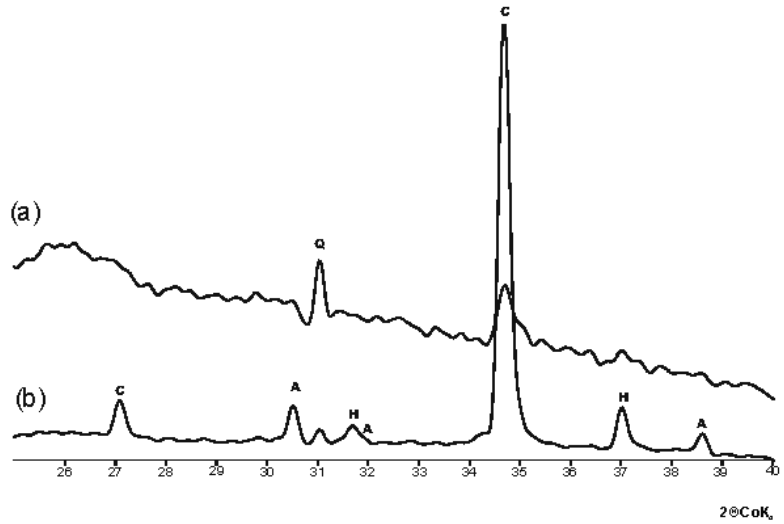

Figure 8. X-ray diffraction spectra of mineral components from mat zones 1 (a) and 2 (b). C - Mg-calcite, A - aragonite, H - halite, Q - quartz (sand grains).

The presence of ultra small high Mg-calcite particles within the two active cyanobacterial layers is related to the high photosynthetic rates observed within these zones. The $CaCO_3$ saturation level within cyanobacterial mats and surrounding waters seems to be the major factor controlling the calcification potential of microbial mats (Simkiss 1986; Kempe and Kazmierczak 1990). Table 1 shows saturation indices (SI) calculated for the cultured mats and the original sediment. The calculations indicate that both the overlaying water and the mat interiors down to the depth of calcium carbonate precipitation (~2.5 mm) were extremely supersaturated with respect to the solubility product of calcite, aragonite and dolomite. The supersaturation was much lower in the original sediments from Nivå Bay, Øresund (Table 1), mostly due to its significantly lower pH, as compared with the apparent pH increase in the culture medium during the mat growth. SI values measured in various natural settings sustaining calcifying benthic cyanobacterial mats (e.g. Kempe and Kazmierczak 1990; Merz-Preiß] and Riding 1999) have shown that SI >0.8 is the environmental saturation threshold necessary for inducing $CaCO_3$ precipitation (calcite or aragonite) by living cyanobacterial mats. The $CaCO_3$ saturation in the natural environment of the studied mats (as in the majority of other "normal"marine environments) is below this value and therefore cannot support their *in vivo* calcification.

Highly viscous media are known to influence the kinetics of calcium carbonate crystallization by slowing the ion diffusion rate (Given and Wilkinson 1985). Calcite precipitation instead of aragonite is favored in such a situation (Given and Wilkinson 1985; Buczynski and Chafetz 1991). The high viscosity of the exopolymers can explain the extremely small size and spherical shapes of high Mg-calcite grains precipitated in the active cyanobacterial layers *in vivo*. Amorphous $CaCO_3$ nanoparticles in more liquid media are rather unstable and quickly transform into macrocrystals (Cölfen and Antonietti 1998; Cölfen 2001).

4.2.2 Calcium carbonate precipitation associated with degrading cyanobacteria

The second mode of calcium carbonate precipitation was associated with degradation of cyanobacterial biomass in zones containing purple bacteria and heterotrophic bacteria (Fig. 4). The larger dimensions of the carbonate particles in this zone and their mixed high Mg-calcite/aragonite mineralogy, is probably related to a less viscous precipitation medium, where amorphous precursor particles transformed faster into superstructured grains composed of ordered nanocrystals (Cölfen 2001; Cölfen and Antonietti 1998). The admixture of aragonite in the high Mg-calcite that formed the bulk of the

grains in the two uppermost purple zones, and particularly the presence of pure aragonitic bodies in zone 6, is in accordance with a less viscous precipitation microenvironment as has been postulated for such grain morphologies by Buczynski and Chafetz (1991).

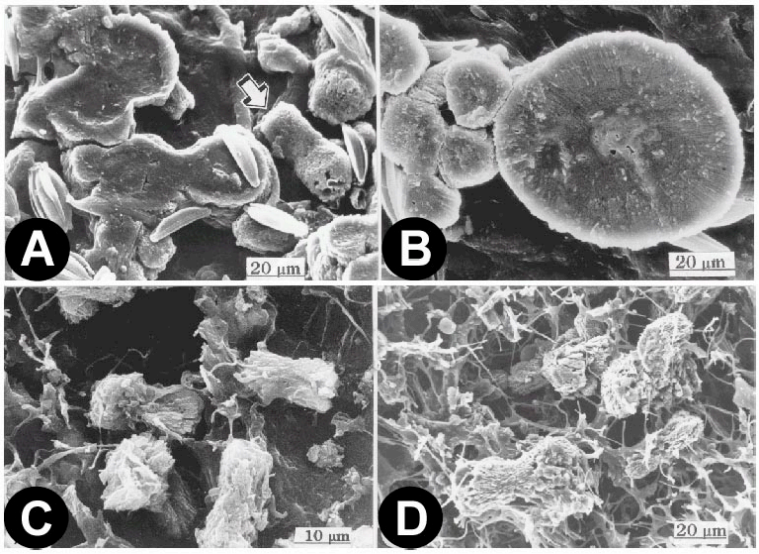

Figure 9. (A) Examples of coalesced Mg-calcite/aragonite hemispheres associated with peanut shaped bodies (arrow); note also numerous frustules of diatoms (*Navicula*). (B) A group of hemispheres showing significant size differences. (C, D) - Examples of imperfect Mg-calcite/aragonite peanut shaped particles irregularly distributed within felt-like remnants of cyanobacterial sheaths (C, from zone 2; D, from zone 4 in Fig. 1). All from a ~2 year old mat.

Bacterial mediation has been suggested instrumental in the formation of $CaCO_3$ precipitates obtained from cyanobacterial mats decaying in calcium rich solutions (Buczynski and Chafetz 1991; Chafetz and Buczynski 1992). Particle morphologies produced in these experiments are strikingly similar, if not identical, to those generated in our artificial mats. Very similar $CaCO_3$ particles have also been found in cultures of heterotrophic bacteria growing in media with calcium carbonate supersaturation (Morita 1980; Riege *et al.* 1991; Rivadeneyra *et al.* 1998; Gonzáles-Muñoz *et al.* 2000; Knorre and Krumbein 2000; Warren *et al.* 2001). However, neither of these studies provided direct evidence for an active participation of bacteria in $CaCO_3$ precipitation, and a whole spectrum of almost identical $CaCO_3$ morphs was obtained from sterile solutions supersaturated with calcium carbonate (Tai and Chen 1998); in particular when polymers were added (Cölfen and Antonietti 1998; Cölfen 2001).

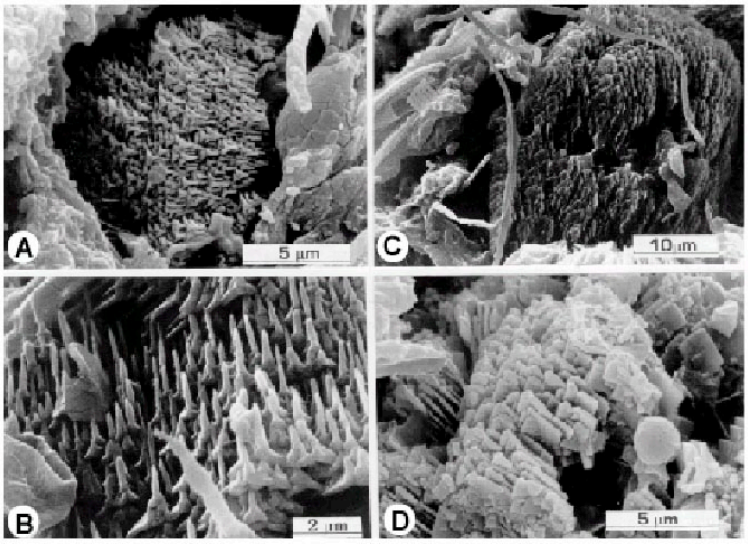

Figure 10. (A, B) Aggregates of dagger-like aragonite crystals. (C, D) Aggregates of platelet rhombic aragonite crystals. All from zone 6 (see Fig. 4) of a ~3 year old mat.

Thus, the role of bacteria in $CaCO_3$ precipitation in the mat could be to supply the supersaturated medium with polymers effective in crystallization control, and, in some cases, to serve as a nucleation centers for the $CaCO_3$ crystals. Furthermore, bacteriolysis of cyanobacterial biomass may significantly increase calcium saturation levels inside mats by releasing Ca^{2+} and Mg^{2+} cations concentrated in cyanobacterial sheaths and EPS (Somers and Brown 1978; Amemiya and Nakayama 1984; Decho 1990). This process may be of key importance in $CaCO_3$ precipitation both in lacustrine and marine cyanobacterial mats (Kazmierczak and Kempe 1998; Stal 2000; Paerl *et al*. 2001). The existence of two different $CaCO_3$ precipitating environments in the artificial mats was also evident from the stable carbon isotope analysis of the various $CaCO_3$ layers. Layers generated in the living cyanobacterial zones showed $\delta^{13}C$ values ~2‰ heavier than in layers of decaying cyanobacterial biomass. In accordance with the stable carbon isotope fractionation within living cyanobacterial mats, i.e. preferential photosynthetic uptake of ^{12}C from the inorganic carbon pool (Calder and Parker 1973; Miller et al. 1990), this confirms that the carbonate species used for $CaCO_3$ precipitation must have been relatively enriched in ^{13}C. In turn, the relatively lighter $\delta^{13}C$ values characterizing the $CaCO_3$ generated in the zones with purple and heterotrophic bacteria suggest input to the inorganic carbon pool of lighter carbon from respiration, i.e. remineralization of cyanobacterial biomass.

Table 1. Hydrochemistry and the carbonate system in the artificial mat (A and B) and in the Nivå Bay, Øresund, Denmark (the origin of precursor material for the artificial mats).

Artificial mats

A) Calculated for S = 21‰ and T = 20ºC Ca: 6.0; Mg: 31.8; K: 5.16; Na: 270.9; SO_4: 15.6 (all mmol/l)

	Day			Night	
	above mat	1 mm depth	2 mm depth	1 mm depth	2 mm depth
PH	8.54	8.82	8.73	8.25	8.26
A_c	9.60	10.10	6.58	10.10	6.58
$SI_{Calcite}$	1.48	1.73	1.48	1.18	1.00
$SI_{Aragonite}$	1.33	1.58	1.33	1.03	8.85
$SI_{Dolomite}$	3.79	4.27	3.78	3.11	2.76
PCO_2	3.04	3.35	3.43	2.72	2.92

B) Calculated for S = 27‰ and T = 20ºC Ca: 12.6; Mg: 39.2; K: 4.57; Na: 259.4; SO_4: 14.6 (all mmol/l)

	Day			Night	
	above mat	1 mm depth	2 mm depth	1 mm depth	2 mm depth
PH	8.54	8.82	8.73	8.25	8.26
A_c	9.60	10.10	6.58	10.10	6.58
$SI_{Calcite}$	1.77	2.01	1.77	1.48	1.30
$SI_{Aragonite}$	1.62	1.87	1.62	1.33	1.45
$SI_{Dolomite}$	4.14	4.63	4.13	3.48	3.12
PCO_2	3.07	3.38	3.46	2.75	2.95

Nivå Bay

S = 22 ‰ and T = 15ºC; Ca: 6.3; Mg: 33.3; K: 6.3; Na: 295.4; SO_4: 17.6 (all mmol/l)

A_c	8.49	mmol/l	$SI_{Calcite}$	0.67
PH	7.80		$SI_{Aragonite}$	0.52
PCO_2	2.35		$SI_{Dolomite}$	2.00

S = salinity; T = temperature; Ac = carbonate alkalinity (mmol/l); pCO_2 = partial pressure of CO_2. Saturation Indices (SI) were calculated according to the formula:
$SI = \log ([Ca^{2+}] \times [CO_3^{2-}]/K)$ with the software PHREEQE (Parkhurst et al. 1980).

5. SUMMARY

The induction of prolific microbial mat growth by removal of fauna shows that grazing and bioturbation are major controlling factors preventing microbial mat development in the majority of extant benthic environments. The integrity and structure of microbial mats is regulated by strong gradients of light and essential chemicals and by hydrodynamic factors affecting diffusive fluxes and boundary layers. When kept under constant temperature, flow, salinity, and light-dark periods, complex laminations of phototrophic microorganisms and EPS developed in the mat. The EPS structure in combination with the metabolic activity of phototrophs and heterotrophs lead to calcification within certain microzones, each with characteristic sizes and shapes of carbonate. Faunal grazing and especially bioturbation destroys and prevents formation of such patterns.

Artificial cyanobacterial mats induced by removal of fauna represent a simple to use model system for studying the microbial ecology and biogeochemistry of microbial mat formation and development. The mats exhibit the structure and microenvironment of natural mats, and carbon, sulfur and oxygen cycling within the artificial mats is similar to natural ones. Future studies should focus on how the boundary conditions for incubation after removal of fauna affect the composition and structure of developing microbial mats. Also the distribution and dynamics of intermediate sulfide oxidation products and of iron and nitrogen species warrant more investigation. Especially, the microenvironmental controls of calcification potential in the mats under different boundary conditions should be investigated in more detail; e.g. with Ca^{2+} microsensors, which have proven valuable tools in studies of calcifying symbioses (DeBeer *et al.* 2000; Köhler-Rink and Kühl 2000) and biofilms (Hartley *et al.* 1996). The described mats are still actively growing, and we would be happy to share moderate amounts of samples with interested colleagues.

6. ACKNOWLEDGEMENTS

Our studies were funded by the Danish Natural Science Research Council (MK and TF) and the Foundation for Polish Science (JK). Thanks are extended to I. Duun, A. Glud, S. Kempe, C. Kulicki, M. Kuzniarski, B. Lacka, and K. Malkowski for technical assistance and discussions. We thank Wolfgang Krumbein for hosting an excellent workshop on microbial mats and for taking the initiative to this book.

REFERENCES

Abed, R.M.M. and Garcia-Pichel, F. (2001) Long-term compositional changes after transplant in a microbial mat cyanobacterial community revealed using a polyphasic approach. *Environ. Microbiol.* 3, 53-62.

Amemiya,Y. and Nakayama, O. (1984) The chemical composition and metal adsorption capacity of the sheath material isolated from *Microcystis*, Cyanobacteria. *Jap. J. Limnol.* 45, 187-193.

Bauld, J. (1981) Occurrence of benthic microbial mats in saline lakes. *Hydrobiologia* 81, 87-111.

Bauld, J., D'Amelio, E., and Farmer, J.D. (1992) Modern microbial mats. In: Schopf, J.W. and Klein, C. (eds.), *The Proterozoic Biosphere*. Cambridge Univ. Press, New York, pp. 261-269.

Bebout, B. M., Carpenter, S., Des Marais, D. J., and 12 co-authors (2002) Long-term manipulations of intact microbial mat communities in a greenhouse collaboratory: Simulating Earths present and past field environments. Astrobiology 2, 383-402.

Buczynski, C. and Chafetz, H.S. (1991) Habit of bacterially induced precipitates of calcium carbonate and the influence of medium viscosity on mineralogy. *J. Sed. Petrol*. 61, 226-233.

Calder, J.A. and Parker, P.L. (1973) Geochemical implications of induced changes in C13 fractionation by blue-green algae. *Geochim. Cosmochim. Acta* 37, 133-140.

Canfield, D.E. and DesMarais, D.J. (1993) Biogeochemical cycles of carbon, sulfur, and free oxygen in a microbial mat. *Geochim. Cosmochim. Acta* 57, 3971-3984.

Chafetz, H.S. and Buczynski, C. (1992) Bacterially induced lithification of microbial mats. *Palaios* 7, 277-293.

Cölfen, H. (2001) Double-hydrophilic block copolymers: Synthesis and application as novel surfactants and crystal growth modifiers. *Macromol. Rapid Commun*. 22, 219-252.

Cölfen, H. and Antonietti, M. (1998) Crystal design of calcium carbonate microparticles using double-hydrophilic block copolymers. *Langmuir* 4, 582-589.

Davies, G.R. (1970) Algal-laminated sediments, Gladstone Embayment, Shark Bay, Western Australia. *Am. Soc. Petr. Geol. Mem.* 13, 169-205.

Decho, A. (1990) Microbial exopolymer secretions in ocean environments: their role(s) in foodwebs and marine processes. *Oceanogr. Mar. Biol. Annu. Rev.* 28, 73-154.

DeBeer, D., Kühl, M., Stambler, N., and Vaki, L. (2000) A microsensor study of light enhanced Ca^{2+} uptake and photosynthesis in the reef-building coral *Favia* sp. *Mar. Ecol. Progr. Ser.* 194, 75-85.

Des Marais, D.J. (1995) The biogeochemistry of hypersaline microbial mats. *Adv. Microb. Ecol.* 14, 251-274.

Dravis, J.J. (1983) Hardened subtidal stromatolites, Bahamas. *Science* 219, 385-387.

Farmer, J. (1992) Grazing and bioturbation in modern microbial mats. In: Schopf, J.W. and Klein, C. (eds.), *The proterozoic biosphere*. Cambridge Univ. Press, New York, pp. 295-297.

Fenchel, T. (1998a) Formation of laminated cyanobacterial mats in the absence of benthic fauna. *Aq. Microb. Ecol*. 14, 235-240.

Fenchel, T. (1998b) Artificial cyanobacterial mats: structure and composition of the biota. *Aq. Microb. Ecol*. 14, 241-251.

Fenchel, T. (1998c) Artificial cyanobacterial mats: cycling of C, O, and S. *Aq. Microb. Ecol*. 14, 253-259.

Fenchel, T. and Kühl, M. (2000) Artificial cyanobacterial mats: growth, structure, and vertical zonation patterns. *Microb. Ecol*. 40, 85-93.

Ferris, F.G., Wiese, R.G., and Fyfe, W.S. (1994) Precipitation of carbonate minerals by microorganisms: Implications for silicate weathering and the global carbon dioxide budget. *Geomicrobiol. J.* 12, 1-13.

Ferris, F.G., Thompson, J.B., and Beveridge, T.J. (1997) Modern freshwater microbialites from Kelly Lake, British Columbia, Canada. *Palaios* 12, 213-219.

Garret, P. (1970) Phanerozoic stromatolites: noncompetitive restriction by grazing and burrowing animals. *Science* 169, 171-173.

van Gemerden, H., Tughan, C.S., de Wit, R., and Herbert, R.A. (1989) Laminated microbial ecosystems on sheltered beaches in Scapa Flow, Orkney Islands. *FEMS Microbiol. Ecol.* 62, 87-102.

van Gemerden, H. (1993) Microbial mats: a joint venture. *Mar. Geol.* 113, 3-25.

Gerdes, G., Spira, J., and Dimentman C. (1985) The fauna of the Gavish Sabkha and the Solar Lake – a comparative study. In: G.M. Friedman and W.E. Krumbein (eds.*), Hypersaline Ecosystems: The Gavish Sabkha*, Springer, New York, pp. 322-345.

Gerdes, G. and Krumbein, W.E. (1987) Biolaminated deposits. In: S. Bhattacharji, G.M. Friedman, H.J. Neugebauer, and A. Seilacher (eds.), *Lecture notes in Earth sciences*, Springer, Heidelberg, Vol. 9, 1-183.

Giani, D., Seeler, J., Giani, L., and Krumbein, W.E. (1989) Microbial mats and physicochemistry in a saltern in the Bretagne (France) and in a laboratory scale saltern model. *FEMS Microbiol. Ecol.* 62, 151-162.

Ginsburg, R.N. (1991) Controversies about stromatolites: Vices and virtues. In: D.W. Müller, J.A. MacKenzie, and H. Weissert (eds.), *Controversies in Modern Geology*, Academic Press, London, pp. 25-36.

Given, R.K. and Wilkinson, B.H. (1985) Kinetic control of morphology, composition, and mineralogy of abiotic sedimentary carbonates. *J. Sed. Petrology* 55, 109-119.

González-Muñoz, M.T., Ben Chekroun, K., Ben Aboud, A., Arias, J.M., and Rodriguez-Gallego, M. (2000) Bacterially induced Mg-calcite formation: role of Mg^{2+} in development of crystal morphology. *J. Sed. Res*. 70, 559-564.

Grotzinger, J.P. and Knoll, A.H. (1999) Stromatolites in Precambrian carbonates: evolutionary mileposts or environmental dipstics? *Ann. Rev. Earth Planet. Sci.* 27, 313-358.

Hartley, A.M., House, W.A., Leadbeater, B.S.C., and Callow, M.E. (1996) The use of microelectrodes to study the precipitation of calcite upon algal biofilms. *J.Coll. Interf. Sci.* 183, 498-505.

Javor, B.J. and Castenholz, R.W. (1984) Invertebrate grazers of microbial mats, Laguna Guerrero Negro, Mexico. In: Y. Cohen, R.W. Castenholz, and H.A. Halvorson (eds.), *Microbial Mats: Stromatolites*. Alan R. Liss, New York, pp. 85-94.

Jørgensen, B.B., Revsbech, N.P., and Cohen, Y. (1983) Photosynthesis and structure of benthic microbial mats: microelectrode and SEM studies of four cyanobacterial communities. *Limnol. Oceanogr.* 28, 1075-1093.

Jørgensen, B.B. and Nelson, D.C. (1988) Bacterial zonation, photosynthesis, and spectral light distribution in hot spring microbial mats of Iceland. *Microb. Ecol.* 16, 133-147.

Jørgensen, B.B. (1989) Light penetration, absorption, and action spectra in cyanobacterial mats. In: Y. Cohen and E. Rosenberg (eds.), *Microbial Mats: Physiological Ecology of Benthic Microbial Communities*. Am. Soc. Microbiol., Washington D.C., pp. 123-137.

Kazmierczak, J. and Kempe, S. (1998) Bacterial spherulites associated with coccoid cyanobacterial microbialites from Lake Van, Turkey: Clues for the origin of ooids. In: J.C. Canaveras, M.A. Garcia del Cura, and J. Soria (eds.), *Abstracts of the 15th International Sedimentological Congress*, Universidad de Alicante Press, Alicante, pp. 465-466.

Kazmierczak, J., Coleman, M.L., Gruszczynski, M., and Kempe, S. (1996) Cyanobacterial key to the genesis of micritic and peloidal limestones in ancient seas. *Acta Palaeont. Pol.* 41, 319-338.

Kempe, S. and Kazmierczak, J. (1990) Calcium carbonate supersaturation and the formation of *in situ* calcified stromatolites. In: V. Ittekkot, S. Kempe, W. Michaelis, and A. Spitzy (eds.), *Facets of Modern Biogeochemistry*, Springer, Berlin, pp. 255-278.

Kempe, S., Kazmierczak, J., Landmann, G., Konuk, T., Reimer, A., and Lipp, A. (1991) Largest known microbialites discovered in Lake Van, Turkey. *Nature (London)* 349, 605-608.

Knorre, H.v. and Krumbein, W.E. (2000) Bacterial calcification. In: R.E. Riding and S.M. Awramik (eds.), *Microbial Sediments*, Springer-Verlag, Berlin, pp. 25-31.

Köhler-Rink, S. and Kühl, M. (2000) Microsensor analysis of photosynthesis and respiration in larger symbiotic foraminifera. 1. The physico-chemical microenvironment of *Amphistegina lobifera*, *Amphisorus hemprichii* and *Marginopora vertebralis*. *Mar. Biol.* 137, 473-486.

Krumbein, W.E., Cohen, Y., and Shilo, M. (1977) Solar Lake (Sinai). 4. Stromatolithic cyanobacterial mats. *Limnol. Oceanogr.* 22, 635-656.

Krumbein, W.E. (1979a) Calcification by bacteria and algae. In: P.A. Trudinger and D.J. Swaine (eds.), *Biogeochemical Cycling of Mineral-Forming Elements*, Elsevier, Amsterdam, pp. 47-68.

Krumbein, W.E. (1979b) Photolithotrophic and chemoorganotrophic activity of bacteria and algae as related to Beachrock formation and degradation (Gulf of Aqaba, Sinai). *Geomicrobiol. J.* 1, 139-203.

Krumbein, W.E., Paterson, D.M., and Stal, L.J. (1994) *Biostabilization of Sediments*. BIS-Verlag, Oldenburg.

Kühl, M., Lassen, C., and Jørgensen, B.B. (1994). Optical properties of microbial mats: light measurements with fiber-optic microprobes. In L. J. Stal and P. Caumette (eds.), *Microbial Mats: Structure, Development and Environmental Significance.* Springer, Berlin, pp. 149-167.

Kühl, M., Glud, R.N., Ploug, H., and Ramsing, N.B. (1996) Microenvironmental control of photosynthesis and photosynthesis-coupled respiration in an epilithic cyanobacterial biofilm. *J. Phycol.* 32, 799-812.

Kühl, M., Lassen, C., and Revsbech, N.P. (1997). A simple light meter for measurements of PAR (400-700 nm) with fiber-optic microprobes: application for P vs. I measurements in microbenthic communities. *Aq. Microb. Ecol.*. 13, 197-207.

Kühl, M. and Fenchel, T. (2000) Bio-optical characteristics and the vertical distribution of photosynthetic pigments and photosynthesis in an artificial cyanobacterial mat. *Microb. Ecol*. 40, 94-103.

Kühl, M. and N.P. Revsbech. (2001) Biogeochemical microsensors for boundary layer studies. In: B.P. Boudreau and B. B. Jørgensen (eds.), *The Benthic Boundary Layer*. Oxford University Press, New York, pp. 180-210.

Logan, B.W. (1961). Cryptozoon and associate stromatolites from the recent of Shark Bay, Western Australia. *J. Geol.* 69, 517-533.

McNamara, K. (1992) *Stromatolites*. Western Australian Museum, Perth.

Merz, M. (1992) The biology of carbonate precipitation by cyanobacteria. *Facies* 26, 81-102.

Merz, M. and Zankl, H. (1993) The influence of the sheath on carbonate precipitation by Cyanobacteria. In: F. Baratollo, P. De Castro and M. Parente (eds.), Studies on Fossil Benthic Algae. *Bolletino della Societa Palaeontologica Italiana*, Special Volume 1, pp. 325-331.

Merz-Preiss, M. and Riding, R. (1999) Cyanobacterial tufa calcification in two freshwater streams: ambient environment, chemical thresholds and biological processes. *Sediment. Geol.* 126, 103-124.

Miller, A.G., Espie, G.S., and Canvin, D.T. (1990) Physiological aspects of CO_2 and HCO_3^- transport by cyanobacteria: a review. *Can. J. Bot*. 68, 1291-1302.

Morita, R.Y. (1980) Calcite precipitation by marine bacteria. *Geomicrobiol. J.* 2, 63-82.

Nübel, U., Garcia-Pichel, F., Kühl, M., and Muyzer, G. (1999) Quantifying microbial diversity: Morphotypes, 16S rRNA genes, and carotenoids of oxygenic phototrophs in microbial mats. *Appl. Environ. Microbiol.* 65, 422-430.

Paerl, H.W., Pinckney, J.L., and Steppe, T. F. (2000) Cyanobacterial-bacterial mat consortia: examining the functional unit of microbial survival and growth in extreme environments. *Environ. Microbiol.* 2, 11-26.

Paerl, H.W., Steppe, T.F., and Reid, R.P. (2001) Bacterially mediated precipitation in marine stromatolites. *Environ. Microbiol.* 3, 123-30.

Parkhurst, D.L., Thorstenson, D.C., and Plummer, L.N. (1980) PHREEQE – A computer program for geochemical calculations. *U.S. Geol. Surv. Wat. Res. Investig.* 80-96, 1-210.

Pentecost, A. and Bauld, J. (1988) Nucleation of calcite on the sheaths of cyanobacteria using a simple diffusion cell. *Geomicrobiol. J.* 6, 129-135.

Pringault, O. and Garcia-Pichel, F. (2000) Monitoring of oxygenic and anoxygenic photosynthesis in a unicyanobacterial biofilm, grown in a benthic gradient chamber. *FEMS Microbiol. Ecol.* 33, 251-258.

Pringault, O., de Wit, R., and Caumette, P. (1996) A benthic gradient chamber for culturing phototrophic sulfur bacteria on reconstituted sediments. *FEMS Microbiol. Ecol.* 20, 237-250.

Pringault, O., de Wit, R., and Kühl, M. (1999a) A microsensor study of the interaction between purple sulfur and green bacteria in experimental benthic gradients. *Microb. Ecol.* 37, 173-184.

Pringault, O., Epping, E., Guyoneaud R., Khalili, A., and Kühl, M. (1999b) Dynamics of anoxygenic photosynthesis in an experimental green sulphur bacteria biofilm. *Environ. Microbiol.* 1, 295-305.

Reid, R.P., Visscher, P.T., Decho, A.W., Stolz, J.F., Bebout, B.M., Dupraz, C., Macintyre, I.G., Paerl, H.W., Pinkney, J.L., Prufert-Bebout, L., Steppe, T.F., and DesMarais, D.J. (2000) The role of microbes in accretion, lamination and early lithification of modern stromatolites. *Nature* (London) 406, 989-992.

Revsbech, N.P., Jørgensen, B.B., Blackburn, T.H., and Cohen, Y. (1983) Microelectrode studies of the photosynthesis and O_2, H_2S, and pH profiles of a microbial mat. *Limnol. Oceanogr.* 28, 1062-1074.

Riege, H., Gerdes, G., and Krumbein, W.E. (1991) Contribution of heterotrophic bacteria to the formation of $CaCO_3$-aggregates in hypersaline microbial mats. *Kieler Meeresforsch*. Sonderh. 8, 168-172.

Riding, R. (2000) Microbial carbonates: the geological record of calcified bacterial-algal mats and biofilms. *Sedimentology* 47 (Suppl.), 179-214.

Riding, R., Awramik, S.M., Winsborough, B.M., Griffin, K.M., and Dill, R.F. (1991) Bahamian giant stromatolites - microbial composition of surface mats. *Geol. Mag.* 128, 227-234.

Rivadeneyra, M.A., Delgado, G., Ramos-Cormenzana, A., and Delgado, R. (1998) Biomineralization of carbonates by *Halomonas euryhalina* in solid and liquid media with different salinities: crystal formation sequence. *Res. Microbiol.* 149, 277-287.

Schopf, J.W. and Klein, C. (eds.) (1992) *The Proterozoic Biosphere*. Cambridge Univ. Press, Cambridge.

Schopf, J.W. (2000) The fossil record: tracing the roots of the cyanobacterial lineage. In: B.A. Whitton and M. Potts (eds.), *The Ecology of Cyanobacteria,* Kluwer Acad. Publ., Dordrecht, pp. 13-35.

Schultze-Lam, S., Ferris, F.G., Sherwood-Lollar, B., and Gerits, J.P. (1996) Ultrastructure and seasonal growth patterns of microbial mats in a temperate climate saline-alkaline lake: Goodenough Lake, British Columbia, Canada. *Can. J. Microbiol.* 42, 147-161.

Schwartz, H.-U., Einselle, G., and Herm, D. (1975) Quartz-sandy, grazing contoured stromatolites from coastal embayments of Mauritania, West Africa. *Sedimentology* 22, 529-561.

Simkiss, K. (1986) The processes of biomineralization in lower plants and animals. In: B.S.C Leadbeater and R. Riding (eds.), *Biomineralization in Lower Plants and Animals*, Oxford Univ. Press, Oxford, pp.19-36.

Somers, G.F. and Brown, M. (1978) The affinity of trichomes of blue-green algae for calcium ions. *Estuaries* 1, 17-28.

Stal, L.J., van Gemerden, H., and Krumbein, W.E. (1985) Structure and development of a benthic marine microbial mat. *FEMS Microbiol. Ecol.* 31, 111-125.

Stal, L.J. (2000) Cyanobacterial mats and stromatolites. In: B. A. Whitton & M. Potts (eds.), *The Ecology of Cyanobacteria,* Kluver Acad. Publ., Dordrecht, pp. 61-120.

Tai, C.Y.and Chen, F.-B. (1998) Polymorphism of $CaCO_3$ precipitated in a constant-composition environment. *AIChE J.* 44, 1790-1798.

Thar, R., Kühl, M., and Holst, G. (2001) A fiber-optic fluorometer for microscale mapping of photosynthetic pigments in microbial communities. *Appl. Environ. Microbiol.* 67, 2823-2828.

Walter, M.R. and Heys, G.R. (1985) Links between the rise of metazoa and the decline of stromatolites. *Precambrian Res.* 29, 149-174.

Warren, L.A., Maurice, P.A., Parmar, N., and Ferris, F.G. (2001) Microbially mediated calcium carbonate precipitation: Implications for interpreting calcite precipitation and for solid-phase capture of inorganic contaminants. *Geomicrobiol. J.* 18, 91-115.

Wickstrom, C.E. and Wiegert, R.E. (1980) Response of thermal algal-bacterial mat to grazing by brine flies. *Microb. Ecol.* 6, 313-315.

Wickstrom, C.E and Castenholz R.W. (1985) Dynamics of cyanobacterial and ostracod interactions in an Oregon hot spring. *Ecology* 66, 1024-1041.

Wieland, A. and Kühl, M. (2000) Short-term temperature effects on oxygen and sulfide cycling in a hyper-saline cyanobacterial mat (Solar Lake, Egypt). *Mar. Ecol. Progr. Ser.* 197, 87-102.